MORPHODYNAMICS OF THE CÁVADO ESTUARY INLET (NW PORTUGAL)

E. Loureiro*, H. Granja** and J. L. S. Pinho***

*University of Minho, Earth Sciences Department, Campus of Gualtar, 4710-057 Braga, Portugal (eduardo.marinha@clix.pt)
**University of Minho, Earth Sciences Department, Campus of Gualtar, 4710-057 Braga, Portugal (hgranja@dct.uminho.pt)
***University of Minho, Civil Engineering Department, Campus of Gualtar, 4710-057 Braga, Portugal (jpinho@civil.uminho.pt)

ABSTRACT

The Cávado estuary inlet is situated in the coastal zone of Esposende (NW Portugal) where sandy beaches have migrated inland and thinned, and cliffs have retreated rapidly over the last years. The coastal zone of Esposende extends over 15 km from the Neiva River until Apúlia.

The coastal segment of Esposende can be considered of mixed energy and wave-dominated type, according to DAVIS and HAYES (1984). The local tide is mesotidal and semidiurnal, with a maximum equinoctial spring tide high-water level of 3.9 m, a minimum low-water level of 0.2 m, and a mean spring tide of 3.49m (data from Instituto Hidrográfico da Marinha).

The inlet is a natural feature of the Cávado estuary, subject to silting up, and enclosed between a breakwater on the northern side and the end of a migrant sandy spit on the southern side. Recently, it was suggested that the best option for decreasing silting-up and increasing navigability, would be to build two breakwaters and artificially manage the inlet. This proposal was not accepted by all concerned and is presently frozen. Behind the spit lies the town of Esposende, and so it is crucial as its natural defence against sea incursions. Several times the sea overwashed the spit, and broke through twice during the last twenty years.

The present study concerns the period between 1991 and 2003. Using the hydrographical maps of 1991, 1992 and 2001, and topo-hydrographic surveys of 2002 and 2003, the sedimentary budget of the inlet, and the morphological changes of the flood and ebb tidal deltas were calculated. Moreover, two hydrodynamic mathematical models and a sediment transport mathematical model were implemented, in order to assess the bottom morphodynamic behaviour at the inlet. The first one is a two-dimensional hydrodynamic (2DH) model that was created using the RMA2 software (WES-HL, 1996). The river stretch considered in this finite elements model begins downstream of the Angelino weir and ends in the Atlantic Ocean.

Key words: hydrodynamics, sediment transport, mathematical modelling

INTRODUCTION

The study of estuaries is of great difficulty since these water systems usually involve complex geometries, hydrodynamics, and transport patterns. In fact, the interface between fresh and salt waters forced by river discharges, tides and wind presents specific characteristics that affect the sand transport patterns that usually form the estuary bottoms. There is a large variability in estuaries depending on differences in tides, river discharges, and the way these factors interact with the topography (DYER, 1997).

Inlets linking estuaries and ocean are very variable in size and shape, due to the patterns and characteristics of bi-directional flow between the ocean and the river. They are a key element of the stability of the estuary, as sediment, salinity, nutrient, and pollutant exchanges between ocean and river go through them.

Bedload transport is quite sensitive to small changes in velocity, such as those brought about by tidal distortion and gravitational circulation (DRUERY, et *al*., 1983). These two mechanisms generate residual bedload flow upstream, in the lower portion of the channel, while fresh, river water drains seaward in the upper portion. Together, these two processes result in a strong net upstream transport of marine sands that forms shoals and flood tidal deltas in the lower estuarine reaches.

Waves breaking on the entrance bars bring considerable volumes of sand into suspension that can be carried into the estuary during flood tide. Much of this sand is flushed back out of the estuary during ebb tide, but a small amount is deposited into the estuary from where it is transported upstream by the net flood tidal flow caused by tidal distortion. Most of the sand transported out of the entrance by floods is deposited on or near the entrance bar from where it is carried to the updrift coastline by a process known as littoral bypassing (BRUUN, 1966).

According to HAYES (1979), most of the sandy bars are located near the mouth in the zones where the action of the waves and the tidal currents is equivalent (mixed energy), (FITZGERALD, 1984). These mouths and their sandy bars show large morphological variations.

All the river mouths situated on the west coast of Portugal show estuaries and inlets. Some of these inlets are totally or partially stabilised by engineering works. This is the case of the Cávado estuary, which inlet has a breakwater on the northern side. The behaviour of this inlet is still poorly known.

SITE DESCRIPTION

The Cávado estuary inlet (Figure 1) is situated in the coastal zone of Esposende (NW Portugal) where sandy beaches have migrated inland and thinned, and cliffs have retreated rapidly over the last years. The coastal zone of Esposende extends over 15 km from the Neiva River until Apúlia. Palaeozoic schists and quartzite outcrops with an approximately NW-SE orientation characterise the nearshore and low-tide area. This coastal segment can be considered of the mixed energy and wave-dominated type, according to DAVIS and HAYES (1984). The local tide is mesotidal and semidiurnal, with a maximum equinoctial spring tide high-water level of 3.9 m, a minimum low-water level of 0.2 m and a mean spring-tide range (MSR) of 3.75m (data from Instituto Hidrográfico da Marinha, 2003). During the period of this study, prevailing winds were from N-NW (38%), S-SW (18%) and W (5%). The main wave climate was from NW (79%) and SW (14%) directions, mostly during fair weather conditions and winter, respectively (data from Departamento de Pilotos do Porto de Viana do Castelo, 2002). Wave conditions are of the oceanic type, with a mean significant wave height (H_s) of 2.12m and period of 9.3s. The maximum wave height during normal winter storms was 4.11m (data from Instituto Hidrográfico da Marinha, 2003). The wave direction is predominantly NW, causing southward longshore drift.

The estuary mouth of the Cávado river is nowadays subject to silting up, and enclosed between a breakwater on the northern side and the end of a migrating sandy spit (Ofir) on the southern side (Figure 1). Recently, it was suggested that the best option for decreasing silting-up and increasing navigability, would be to build two breakwaters and artificially manage the inlet. This proposition was not accepted by all concerned and is now held off. Behind the spit lies the town of Esposende, and so it is crucial as its natural defence against sea incursions. Several times the sea overwashed the spit, and broke through twice during the last twenty years.

The Cávado river inlet is mostly shallow, with a main channel depth ranging between 1 and 3 m in the navigable portion of the system, and about 40m width (N-S). It is E-W oriented, between a breakwater (northern side) and the end of the sandy spit of Ofir (southern side) that is fronted by a large intertidal spit platform.

From the ocean to inland, the main morphological units are: the ebb tidal delta in the entrance of the mouth, a sandy bar with the main axis oriented according to the net ebb flow; the flood tidal delta near the breakwater, a lobate sandy bar that seasonally develops in the inner part of the mouth; the main channel with variable depth (0.5 to 1 m, data of 07/ 2002), and one or two secondary, narrower and shallower channels.

Considering the mean wave breaker-height (H_b= 2.74m) for the study period, the seaward action limit of the littoral drift currents into the estuary inlet were situated at circa 3.5m depth (HARDISLY e LAVER, 1989).

In order to prevent or to mitigate the silting-up and navigability problems, and the erosive and migratory trends of the extreme N of the Ofir spit, it is important to understand the morphodynamic behaviour of the Cávado estuary inlet. This paper represents a step in this direction through an inlet monitoring program (topo-hydrographic surveys, field inspections, wave data acquisition, sediment sampling, analysis of aerial imagery and interpretation of detailed bathymetric data) and the implementation of preliminary mathematical modelling results of the sediment transport at the Cávado River inlet in order to assess the morphodynamic behaviour at the inlet. Bottom morphodynamics are simulated for average river discharges and considering different tidal conditions.

METHODS

The present study covers the period between 1991 and 2003. The methods used in this study consisted of: 1) topo-hydrographic surveys during 2002 and 2003, and bathymetric data analysis of hydrographic maps of 1991, 1992 and 2001; 2) GPS monitoring during July and August of 2003; 3) wave data acquisition; 4) sediment sampling; 5) hydrodynamic parameter calculations; 6) mathematical formulations to implement a hydrodynamic model and sediment transport model.

Topo-hydrographic surveys and bathymetric analysis

All the surveys are referred to ZH level, the national hydrographic level, 2m below mean sea level (MSL), and to Hayford/Gauss Datum. Using the data of the topo-hydrographic surveys and of the bathymetric maps (GORMAN et *al*., 1998), the sedimentary budget and the morphological changes were calculated.

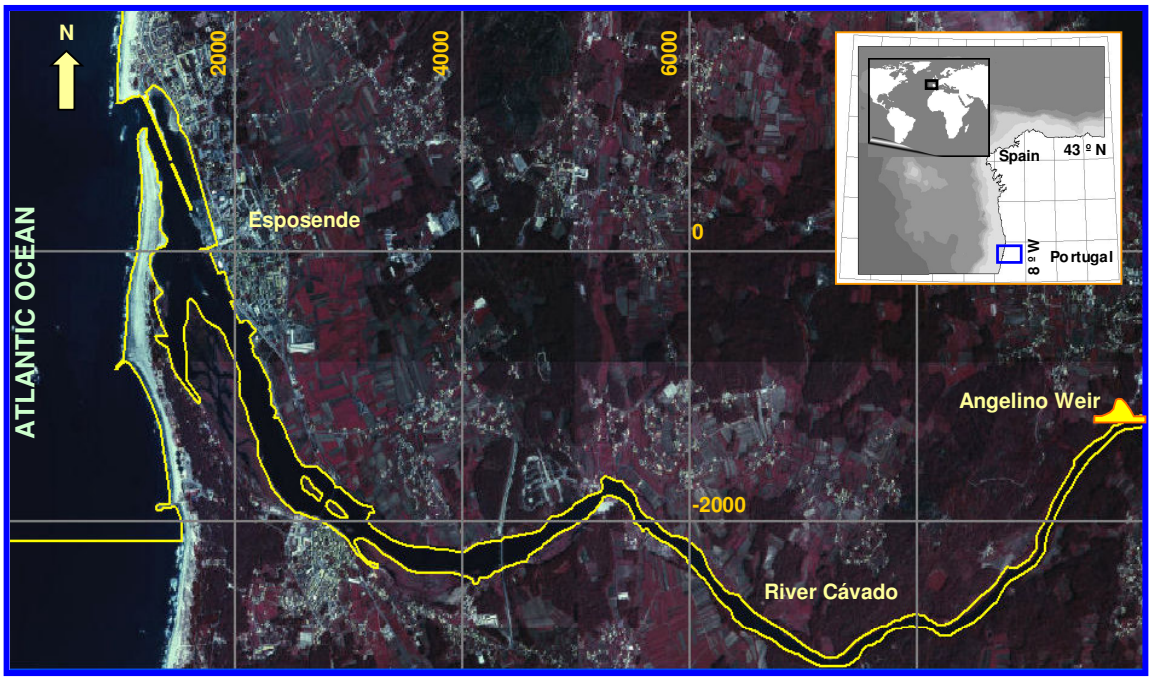

Figure 1- Location of the Cávado River estuary and inlet.

a) Sedimentary budget

During the study period (1991, 1992, 2001, 2002 and 2003), topographic surveys along 4 N-S and 3 E-W lines were made, covering a 400m long and 195m wide area between the breakwater and the extreme N of the spit, to calculate the sedimentary budget at the inlet. The calculation of volumes and profile areas was done with the programs *Surfer version 8.0* and AutoCAD 2000. The volume calculation was made by *Kriging*, using the Trapezoidal, Simpson, and 3/8 of Simpson operation methods. The comparison of the values by the three modes resulted in volumes with a relative error of less than 0.06%.

b) Morphological changes of the tidal delta

Three N-S profiles with about 40m intervals were made in the ebb tidal delta of the Cávado river mouth. These profiles were made in 1991, 1992, 2001, 2002, and 2003, at the Gauss/Hayford coordinate points 145028/508278, 145064/508286, and 145104/508280.

GPS monitoring

During July and August of 2003, the position changes of the ebb tidal delta were monitored with a GPS, and the wave breaker type registration was done.

Wave data

Wave data for 2001 to 2003, obtained from the near offshore buoy of Leixões harbour (Lat = 41° 19' 00" N; Long = 8° 59' 00" W; Depth = 83 meters), were reduced to yearly and monthly averages. Wave breaker height (H_b) calculations used direct statistical averages of significant wave height and wave period records (Instituto Hidrográfico data). Breaker height was estimated in the surf zone, according to KOMAR and GAUGHAN (1972), considering the mean of significant wave height of the month prior to the beach survey (BENAVENTE et al. 2000). The yearly mean of the local tide amplitude was calculated from the Instituto Hidrográfico data.

Sediment sampling

Sediments were sampled on the bar-crest and seaward boundary of the bar. All samples were dry-sieved using 1-phi intervals, and size analyses were made with the software Sedmac (HENRIQUES, 2003), based on the moments method.

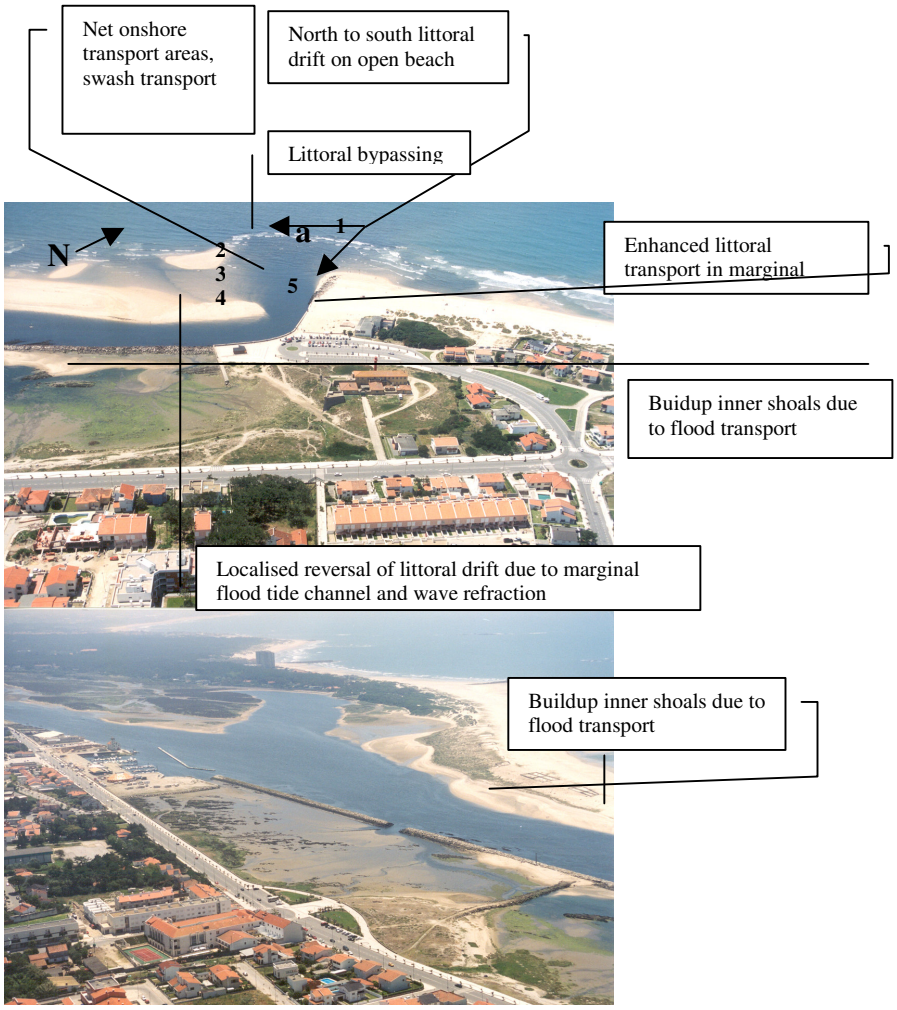

Figure 2 - Sediment pathways in the Cávado estuary mouth.
(1- Wave-dominated processes; 2, 3- Ebb tide-dominated processes; 4- Flood tide-dominated processes; 5- Main ebb tide channel; a- ebb terminal lobe)

Hydrodynamic parameter calculations

The parameters used to characterize the Cávado estuary inlet were: the hydrodynamic coefficient; tidal prism changes; bar changes of the ebb tidal delta; stability rate.

The hydrodynamic coefficient (HAYES, 1979) is given by the relation: yearly mean of the significant wave height / mean tide amplitude.

The tidal prism is the total amount of water flowing into or out of an estuary with movement during the spring tides through the minimum cross-sectional area of the inlet, below mean sea-level (O'BRIEN, 1931, 1969 and JARRET, 1976, in MICHEL, 1993). It depends on the spring tide amplitude and estuary dimensions (GOODWIN, 1996). The relation between the minimum cross-sectional area of the inlet and tidal prism is given by the equation:

$A = C \cdot \Omega^n$, where A = the minimum cross-sectional area (in m^2) of the inlet, below mean sea-level;

Ω = tidal prism during spring tides (in m^3); the minimum cross-sectional area was calculated (GASSIAT,1989). The changes of the minimum cross-sectional area were calculated comparing the same profile in 1991, 1992, 2001, 2002 e 2003.

C and n are two dimensionless constants; according to MICHEL (1993) this relation is given by the equation:

$A = 4\ 10^{-4} \cdot \Omega^{0.9047}$ with a correlation $r^2 = 0.9514$;

The stability rate is the relation tidal prism / total littoral drift (M_{total}) in m^3, corresponding to the total yearly volume of moved sediments by the action of different wave types, and any transport direction. The rate (Ω / M_{total}) represents the type of forcing between the flood tide perpendicular to the coast, and the sedimentary transport parallel to the shore, induced by waves (BRUUN and GERRITZEN, 1960 and BRUUN *et al*., 1974).

With field data and using the KAMPHUIS formula (KAMPHUIS, 1993), the total littoral drift (M_{total}) was estimated to be 2.47×10^6 m^3/year.

Mathematical formulations

Sediment erosion and deposition studies must be based on a fully dynamic model description. In the absence of stratification, the RMA2/SED2D software packages (WES-HL, 1996, WES-HL, 2000) are excellent tools to predict the sand transport patterns. If vertical stratification prevails, a two-dimensional vertical modelling approach or a three-dimensional approach (PINHO, 2001) must be applied.

Hydrodynamic model

The two-dimensional hydrodynamic models in the horizontal plane (2DH) were implemented using the RMA2 software that is based on the finite element method (WES-HL, 1996). This model can be applied for situations where the water flow does not exhibit a significant vertical variation, as was mentioned before, and for situations that are not highly dependent on the waves action. It solves the depth-integrated equations of fluid mass and momentum conservation in two horizontal directions. The forms of the solved equations are:

$$\frac{\partial \eta}{\partial t} + \frac{\partial[(h+\eta)U]}{\partial x} + \frac{\partial[(h+\eta)V]}{\partial y} = 0 \tag{1}$$

$$\frac{\partial U}{\partial t} + U\frac{\partial U}{\partial x} + V\frac{\partial U}{\partial y} = +fV - g\frac{\partial \eta}{\partial x} - \frac{g}{\rho}\frac{\partial \rho}{\partial X}\frac{h+\eta}{2} + \\ + \frac{\rho_a k W_v^2 \cos\varphi}{h+\eta} - \frac{gU\sqrt{U^2+V^2}}{(h+\eta)C^2} + \frac{\varepsilon}{\rho}\left(\frac{\partial^2 U}{\partial x^2} + \frac{\partial^2 U}{\partial y^2}\right) \tag{2}$$

$$\frac{\partial V}{\partial t} + U\frac{\partial V}{\partial x} + V\frac{\partial V}{\partial y} = -fU - g\frac{\partial \eta}{\partial y} - \frac{g}{\rho}\frac{\partial \rho}{\partial y}\frac{h+\eta}{2} + \\ + \frac{\rho_a k W_v^2 sen\varphi}{h+\eta} - \frac{gV\sqrt{U^2+V^2}}{(h+\eta)C^2} + \frac{\varepsilon}{\rho}\left(\frac{\partial^2 V}{\partial x^2} + \frac{\partial^2 V}{\partial y^2}\right) \tag{3}$$

where x and y are the horizontal Cartesian coordinates, t is the time, U and V are the vertical average of the horizontal velocity components, ρ_a is the air density, W_v is the wind velocity, φ is the wind direction, C is the Chezy coefficient and η is the turbulent viscosity coefficient, ρ is the water density, h is water depth, ω is the water surface elevation, k is an empirical wind shear coefficient and f the Coriolis parameter.

Sediment transport model

The sediment transport model, SED2D (WES-HL, 2000) is applied to simulate the sediment transport in aquatic environments. This programme can be applied to clay or sand bed sediments where flow velocities can be considered two-dimensional in the horizontal plane (i.e., the speed and direction can be satisfactorily represented as a depth-averaged velocity). It is useful for both deposition and erosion studies. The program treats two categories of sediment: noncohesive (sand), and cohesive (clay). Both clay and sand may be analyzed, but the model considers a single, effective grain size during each simulation. Therefore, a separate model run is required for each effective grain size. Fall velocity must be prescribed along with the water surface elevations, x-velocity, y-velocity, diffusion coefficients, bed density, critical shear stresses for erosion, erosion rate constants, and critical shear stress for deposition. There are four major computations, using a finite element based numerical method: convection-diffusion governing equation; bed shear stress calculation, bed source/sink term, bed strata discretization.

The basic convection - diffusion equation, reads:

$$\frac{\partial C}{\partial t} + U\frac{\partial C}{\partial x} + V\frac{\partial C}{\partial y} = \frac{\partial}{\partial x}\left(D_x\frac{\partial C}{\partial x}\right) + \frac{\partial}{\partial y}\left(D_y\frac{\partial C}{\partial x}\right) + \alpha_1 C + \alpha_2 \tag{4}$$

where, C is the sediment concentration, D_x is the effective diffusion coefficient in x - direction, D_y is the effective diffusion coefficient in y - direction, α_1 is a coefficient for the source term, and α_2 is the equilibrium concentration portion of the source term.

The bed shear stress is needed to evaluate the bed source-sink terms in the governing equation:

$$\tau_b = \rho\left(u^*\right)^2 \tag{5}$$

where, ρ is the water density and u^* is the shear velocity. Several options are available for computing bed shear stresses using, different formulations for u^* computation: the smooth-wall log velocity profile; the Manning's shear stress equation; a Jonsson-type equation for surface shear stress; and a Bijker-type equation for total shear stress caused by waves and currents.

The form of the bed source term, is the same for deposition and erosion of both sands and clays. Methods of computing the alpha coefficients depend on the sediment type and whether erosion or deposition is occurring. For sand transport, the supply of sediment from the bed (i.e., the sediment reservoir) is controlled by the transport potential of the flow and availability of material in the bed. The bed source term is:

$$S = \frac{C_{eq} - C}{t_c} \tag{6}$$

where, S is the source term, C_{eq} is the equilibrium concentration (transport potential), and t_c is the characteristic time for effecting the transition. The ACKERS-WHITE (1973) transport formula was adopted for calculating C_{eq} for the sand size material.

Sand beds are considered to consist of a sediment reservoir of finite thickness, below which is a non erodible surface. Sediment is added to or removed from the bed at a rate determined by the value of the sink/source term at the previous and present time -steps. The mass rate of exchange with the bed is converted to a volumetric rate of change by the bed porosity parameter.

Model implementation

The regional hydrodynamic model beginning at the open ocean boundary and ending at the first upstream weir, was implemented using a finite element mesh with 6087 triangular quadratic elements (Figure 3b). This mesh was generated considering a minimum interior angle of 25º and a maximum element area constraint of 10000 m^2.

Two open boundaries were considered for the regional hydrodynamic model: an open ocean boundary at the estuary mouth, and an open river boundary at the upstream section of the river. At this location, the river discharges were considered. At the open ocean boundary surface tide elevations were imposed, estimated according to the Topex-Poseidon satellite observation data through the SR95 program (JPL, 1996).

The solution of the regional model was used to establish the open boundary conditions of the local model, by interpolating the obtained hydrodynamic solution to the ocean and river boundaries of the local model. At these locations it was also defined concentrations in the sediment transport model.

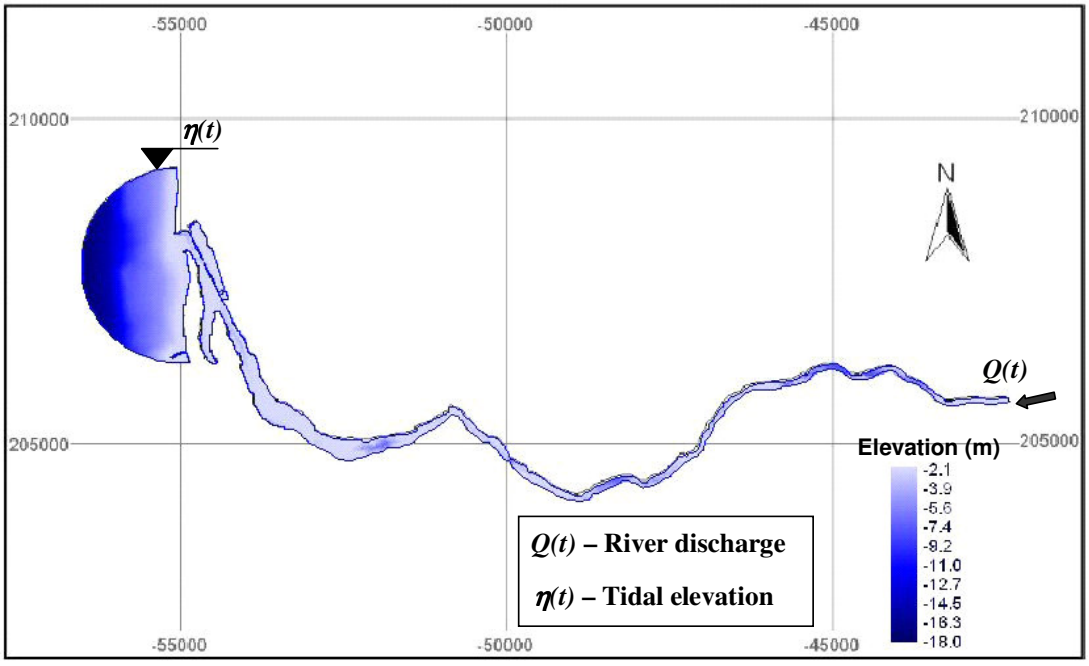

a)

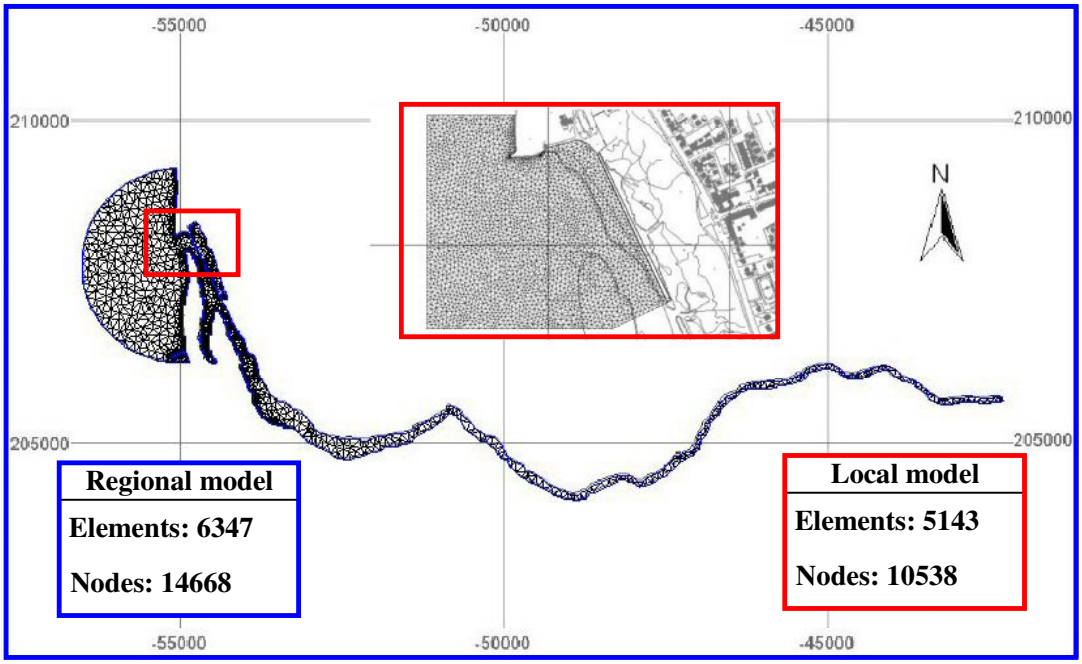

b)

Figure 3 - Hydrodynamic and sediment transport model: **a**) Bathymetry; **b**) 2DH finite element meshes

Model Calibration and validation

Results presented in this work are a first attempt to simulate the sediment transport patterns at the river Cávado inlet. Models calibration and validation requires significant data series that are not yet available. Meanwhile, at this work phase, model parameters were established using values determined in similar studies, available tidal data and other qualitative data observed in the field. Thus, values of 40 $m^{1/3}s^{-1}$ for the Manning-Strickler equation coefficient and 20 m^2s^{-1} for the turbulent viscosity coefficient were adopted for the hydrodynamic models. Figure 4 depicts model computed (lines) and predicted (dots) tidal elevations for Esposende.

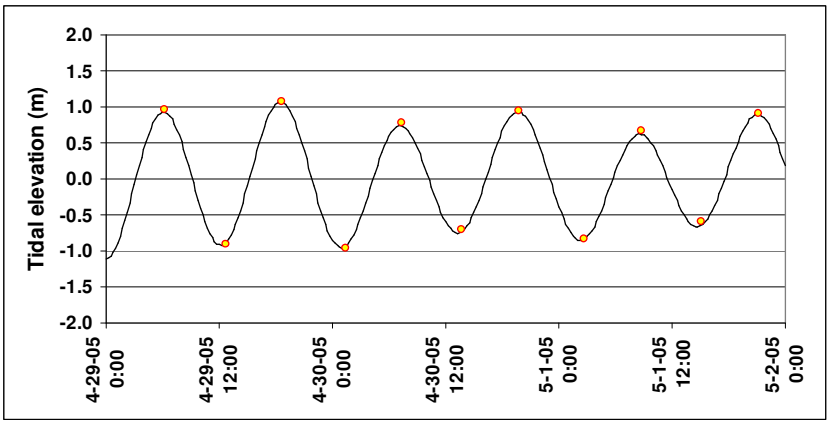

Figure 4 - Hydrodynamic model. Computed (lines) and predicted (dots) tidal elevations at Esposende.

RESULTS

Hydrodynamic coefficient

Considering that the yearly (2002) mean significant height (Hs) was 2.45 m and the mean tidal amplitude (A) was 3.12 m (Instituto Hidrográfico, 2003), the hydrodynamic coefficient (Hs/A) of the Cávado inlet is 0.78. This means it is of mixed energy (wave and tide), with a prevailing action of tidal currents that promote an elongation of the tidal sandy bars of the ebb and flood tidal deltas.

Tidal prism

Data concerning the minimum cross-sectional area, representative of the tidal prism are given in Table 1 and Figure 5.

Using data from 1991, 1992, 2001, 2002 and 2003, tidal prism values were calculated. Data show that the minimum value for the tidal prism was reached in 1991 (5.46 x 10^5 m^3), then increasing until 2001 when the maximum value of 8.61 x 10^6 m^3 was recorded. After 2001, the trend was decreasing again.

Year	Tidal prism (x10^6 m^3)	Minimum cross-sectional area (m^2)
1991	0.55	62
1992	2.12	212
2001(a)	8.61	752
2001(s)	4.55	422
2002	3.41	325
2003	1.70	173

(a)– April ; (s) – September

Table 1- Values of tidal prism and of minimum channel cross-sectional area

Stability rate

With field data and using the KAMPHUIS formula (KAMPHUIS, 1993), the total littoral drift (M_{total}) was estimated to be 2.47x10^6 m^3/year.

The stability rate for the Cávado inlet changed from a minimum of 0.22 (1991) to a maximum of 3.4 (2002), decreasing again until 2003, when the value was 0.6. Considering the average between 1991 and 2003, the stability rate was 1.4. According to MICHEL (1993), this classifies it as a very unstable inlet with easy silting-up. The value of the relation hydrodynamic coefficient (0.78)/ stability rate (1.4), was of 0.44 that shows the inlet instability and tidal currents dominance (STAUBLE, 1993, in MICHEL, 1997).

Bar changes of the ebb tidal delta

Data from sections and profiles of emerged bars (above ZH) are presented in table 2.

	Cross-sectional area (m^2)		
Year	Profile 1	Profile 2	Profile 3
1991	201	370	179
1992	213	348	169
2001	184	176	448
2002	203	216	191
2003	329	419	453

Table 2 –Evolution of the cross-sectional area of the bars of the ebb tidal delta.

Profile 1 – The most westward profile. The bar surface changes are irregular until 2001. From 2001 until 2003, the surface of the bars increases significantly.

Profile 2 – The intermediate profile. Between 1991 and 2001 the area of the bars has been halved, increasing again from 2001 until 2003.

Profile 3 – The most inland profile. The southern end is near the end of the spit. The surface of the bars increases significantly (about 300 m^2) possibly due to the erosion of the beach located north of the breakwater and of the end of sandy spit, here promoted by wave action and flood tidal flows.

Figure 5 shows two sandy ebb bars, with the longest axis oriented NE-SW, in the ebb flow direction, and an E-W oriented channel separating the smaller bar (longest axis ± 50 m) from the larger bar (longest axis ± 100 m). This bar was detached from the west face of the spit by a channel with 0.5 m of maximum depth and about 50 m wide.

The flood sandy bar (Figure 5a) situated south of the breakwater, presented an increase in area and volume from August until October 2001. From December 2001 until January 2002, the bar disappeared. In February

2002, it was formed again and remained in place until April of 2002. The spit platform covers an area of circa 400m by 300m.

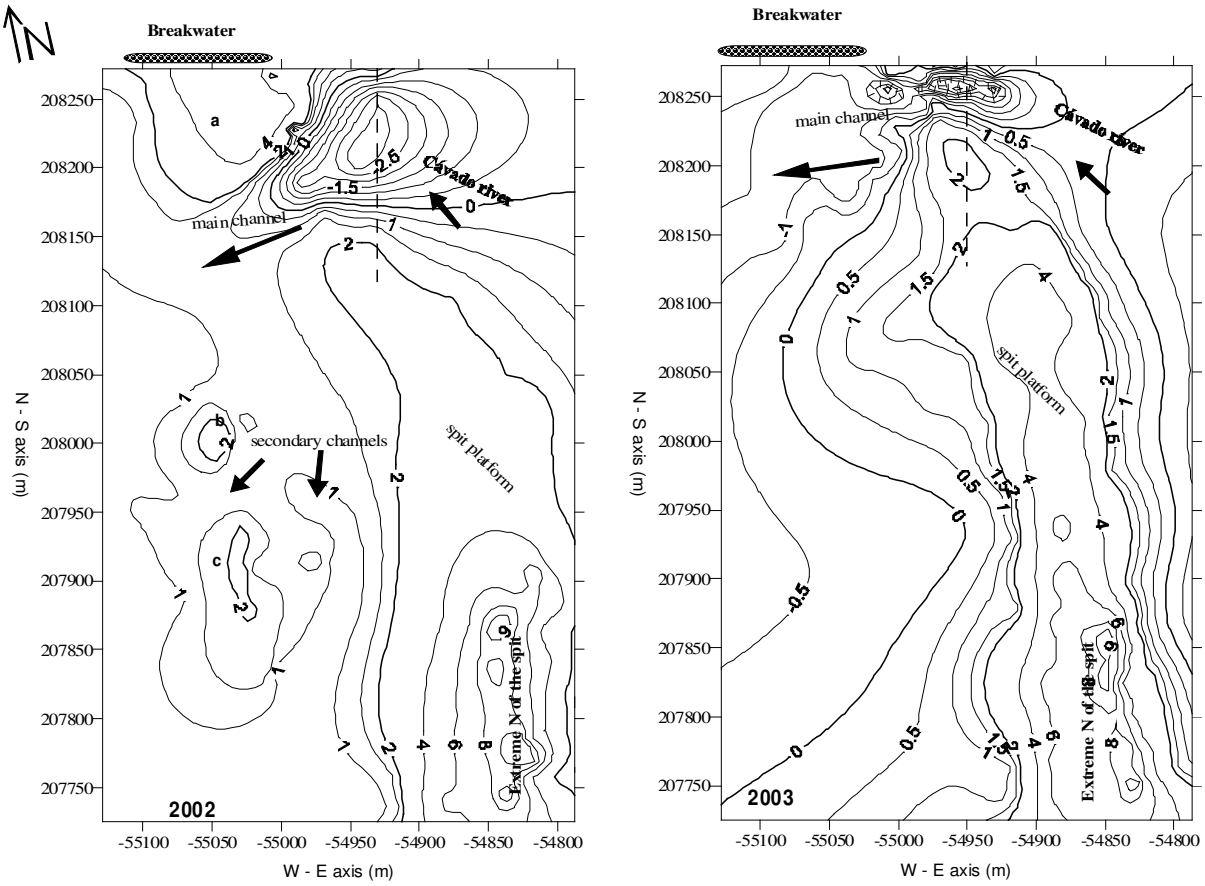

Figure 5 - Contour map of the Cávado estuary mouth (2002 and 2003). The dashed line represents the profile of the cross-sectional area (a, b, c: emerged sandy bars).

During the observation period 2001/2002, the longer axis of the main flood bar changed from an E-W to a NE-SW position.

During the neap tide periods, the bars presented an E-NW to N-SE orientation, an aerial extent reduction, increase of the length of the smaller axis, vertical accretion, and a movement to the end of the spit.

During spring tide periods, the main orientation of the bar was E-W, its extension larger, its height was reduced, and the extension of the smaller axis decreased. The bar ends were sharper. The immerged bar on the north side of the mouth, presented a progression to the south and a vertical accretion, contributing to the increase of silting-up (depth= 0.5 m; sounding data, 11/08/02).

On May 2003, the spit platform was circa 500m by 180m, and its central part presented a vertical accretion of circa 2.5 m, while the oceanwards face presented a height decrease of circa 0.5 to 2.0 m (figure 5). The river face presented an accentuated erosion through the migration from E to W of the 2m contour line.

Sediments and morphological changes

Ebb tidal delta sediments are coarse to very coarse sand (mean 0.85mm) and gravels (mean 40mm).

The monitoring of ebb tidal delta changes, between July and August 2003 show that the bars of the ebb tidal delta have migrated from the north of the mouth to the SSE, close to the end of the spit. The spit platform showed ripple and dune bedforms from waves, swash, and tidal currents.

Sedimentary budget changes at the inlet

Data concerning the areas and volumes are presented in Table 3.

From table 3, it can be seen that the emerged bars (above ZH) presented increasing volumes, while the aerial extension decreased by circa 4 000m^2, until 1992. From 1992 until 2001, the volume and the aerial extension suffered an important decrease. Later on, their volume has increased, the maximum value being attained in 2003. The aerial extension from 1991 until 2003, presented a decreasing trend.

Year	Volume (m^3) Above ZH	Volume (m^3) Below ZH	Area (m^2) Above ZH	Area (m^2) Below ZH
1991	76 224	45	78 476	1 924
1992	103 172	687	73 699	2 681
2001	82 811	18 184	59 557	16 823
2002	138 623	18 617	71 426	12 974
2003	132 164	11 833	66 400	17 999

Table 3 - Volume and area changes of the sandy bars of the Cávado inlet.

The immerged bars (below ZH) from 1991 until 2003, presented an increasing trend in volume and aerial extension.

Globally, between 1991 and 2003, the morphodynamic trend of the Cávado inlet during storm and flooding situations, have shown:

- An increase of the channel depth, contributing to the increase of the tidal prism;
- An increase of the channel width, due to the erosion of the spit end;

During fair weather conditions, the following situations, were present:

- During spring tides, the inlet presented an E-WNW main channel, with variable width, an ebb bar with an E-W oriented long axis and a subtidal bar at the NW, promoting the silting-up of the entrance to the mouth;
- A sedimentary accumulation trend of inner shoals of the estuary;
- During neap tides, the inlet presented an E-W main channel and a secondary NE-SW channel; the ebb bar presented a vertical accretion and a migration to the south in the direction of the end of the spit.

The calculation of the sedimentary volume shows that during the considered period, the subtidal bars were subject to an increasing erosion trend.

Simulated Scenarios

Simulated scenarios were defined considering the river discharge and tide height. Adopted tide heights are representative of the neap-spring tidal range. Two different tide heights were considered: 3.05 m for spring tide and 1.00 m for neap tide. Only the average value for river discharge was adopted. The sediment transport model was used to simulate bed changes under the previous tidal regimes, considering a grain size of 2 mm.

Hydrodynamics

The hydrodynamic simulations were carried out in two steps: in the first step the transient solution between a hydrostatic situation and the dynamic solution was achieved; in the second step two tidal periods were computed using results corresponding to the final time step of the solution previously computed as initial conditions. Although the model calibration process has not been yet completed, it is possible to present some qualitative results (Figure 6).

The maximum current velocities occur at the river channel entrance. Depth average velocity at this location varies from 1.40 ms^{-1} (S1) to 0.40 ms^{-1} (S2) during flood tide and from 3.00 ms^{-1} (S1) to 1.00 ms^{-1} (S2) during ebb tide.

Sediment transport

Figure 7 shows the initial bottom topography considered in the sediment transport model simulations. Results for sediment deposition after 12.5 hours and 25 hours are presented in Figure 8.

For the spring tides simulation, two erosion zones are in evidence: one located south of the Esposende breakwater and the other located at the right of the sandy spit. The sediments deposit preferentially in two zones: the first one located between the sandy spit and the breakwater and the second one located in the ocean in front of the river inlet.

For neap tides, the erosion zones disappear (for the sediment characteristics used in the simulation) and a general tendency for deposition can be observed in the river channel.

For spring tides simulation it is apparent two erosion zones: one located south of the Esposende breakwater and the other located at right of the sandy spit. The sediments deposit preferentially at two zones: the first one

located between the sandy spit and the breakwater and the second one located in the ocean in front of the river inlet.

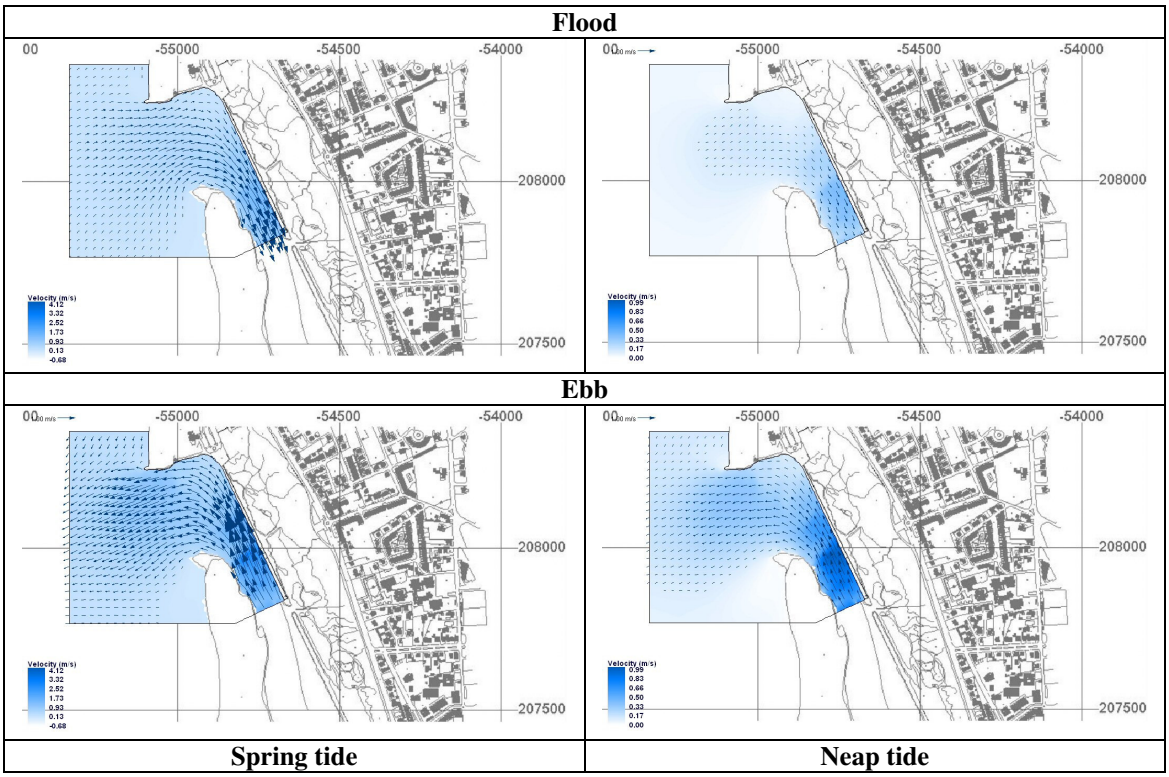

Figure 6. Local hydrodynamic model: highest current velocities during ebb and flood.

For neap tides the erosion zones disappear (for sediment characteristics considered in the simulation) and a general tendency for deposition can be observed in the river channel.

Figure 7. Local sediment transport model: initial bottom topography.

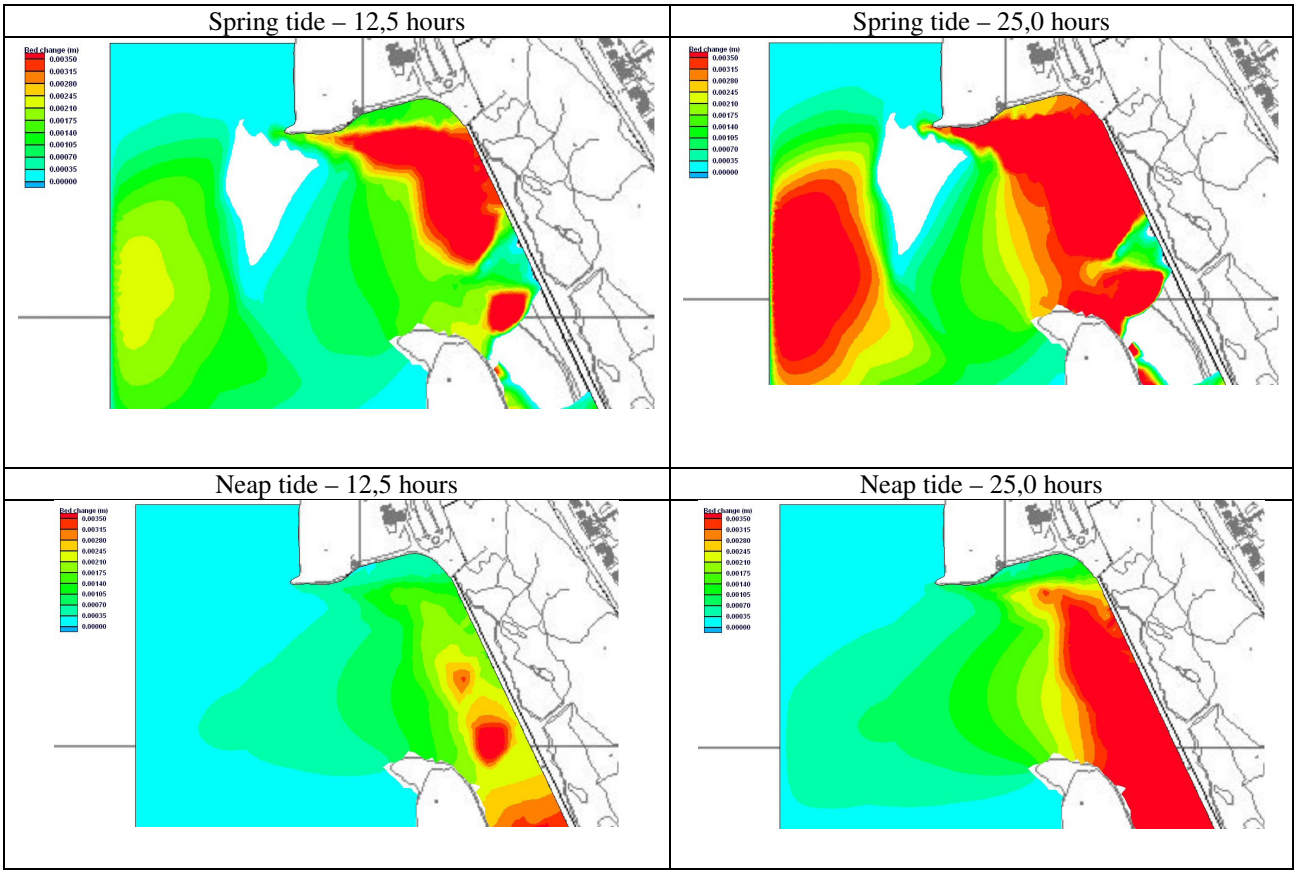

Figure 8. Local sediment transport model: bed change (deposition) under different tidal conditions.

DISCUSSION

During the study period (1991/2003) the main change occurred during 1992, with the breaching of the spit platform and the formation of a new main channel with a width of circa 200m. The erosion of the spit beach and the washovers of the foredune by high wave action during the winter, and the discharge of floodwaters increased the scouring of the ebb currents, contributing to the breaching process of the spit.

Between 1993 and 2000, and apart from the lack of topo-hydrographic data, the periodic visual observation of the spit showed that the wet section did not show significant changes until the end of summer 2000.

On April 2001, the minimum cross-sectional area and tidal prism showed the maximum values. During the winter of 2000/2001, the floods of the Cávado River and storminess waves coincident with the springtides (February 2001) caused the breaching of the spit platform and the formation of new channel. This process contributed to increase the main channel depth and the erosion of the spit platform. Consequently, a decrease of inlet sedimentary budget of circa 20 000m^3 and an increase in the tidal prism and minimum cross-sectional values were observed.

From 2001 to 2003, the minimum cross-sectional area and tidal prism showed a decreasing trend. This situation was related to an increase of the sediment transport into the inlet by wave swash and flood tidal flow and a decrease of the ebb tidal flow resulting of the silting-up of the main channel.

During 2002, the presence of a flood tidal bar on the northern side of the inlet and two well-developed ebb tidal sand bars on the southern side, contributed to the increase of the sedimentary budget, the decrease of the tidal prism and of the minimum cross-sectional area in comparison with 2001 situation. During the neap tide cycle, with the decrease of wave height and prevailing spilling breakers, a vertical accretion of the ebb tidal delta bars and their migration southwards, with later weld of the bar to the spit platform, took place. This movement resulted in a greater refraction of the predominant NW and W waves around the ebb tidal delta. This refraction caused a local reversal in dominant southward longshore sediment transport. During the spring tides of April

2002, the disappearance of the flood delta located south of the breakwater, was possibly due to the gradual transport of part of the sediments inside the estuary by a strong flood current (visual data and fishermen information point to an increase of silting-up of estuary). It is probable in addition, that another part of those sediments has contributed to the accretion by the strong ebb flow action of the ebb tidal delta bars, the aerial extension of which had increased.

Before this situation, the inlet presented an E-WNW main channel of about 100 and 200 m width, a small SW-oriented marginal channel, an ebb bar with E-W-oriented long axis, and a subtidal bar at the NW, promoting the silting-up of the entrance of the inlet. The tidal currents, partly concentrated in the northern channel, caused the erosion of the subtidal bar at the NW. Most of the alongshore sediment is trapped by the outer delta. Consequently, the lack of sediment supply and the southward migration of the marginal channel caused the erosion of the spit platform.

During 2003, the sedimentary volume in the entrance of the inlet showed that relative to 2002, the mouth presented an erosive trend. The existence of only one E-W channel contributed to a greater concentration of ebb flow, constituting a hydrodynamic obstacle to the southward drift, that was then deviated offshore. On the other side, the area of the subtidal bar at the north of the inlet increased, while the ebb bars were eroded by the main action of the waves. South of the inlet, the northwards-oriented reverse drift and the flood flow would have contributed to the vertical accretion of the spit platform, its N-S extension increase and a significant decrease of its width (about 120 m).

Considering that between 1991 and 2003, the tidal prism showed a mean value of 3.40×10^6 m^3, and that in 2003 its value was circa 1.70×10^6 m^3, this means that the inlet presents a strong trend for silting-up presently. In addition, the minimum sectional area has decreased 2.5 times and the channel width decreased 15m, which is not surprising considering that the stability rate of the Cávado mouth is 1.4 (very unstable and easily infilled).

The morphodynamic changes are the result of the intense increasing of flood and ebb tidal currents during the spring tides period associated to the wave processes and sediment amounts. The increase of wave breaker-heights and dominant plunging breakers contribute to the attack of the delta bars and the extreme N of the sandy spit by high-energy waves. The sand enters the main inlet channel by wave action or through marginal channels by tidal currents. Additional sand is transported into the inlet by flood tidal and wave-generated currents over the shallow swash platform that flanks the south side of the main channel.

The morphological and volumetric changes on the emerged and immerged bars seem to show the existence of sand transport between both. The accretion of the emerged bars will essentially result in sediment transport coming from the subtidal area, southwards drift, and erosion of the spit platform. Between 2002 and 2003, the spit platform length increased by circa 100m and its width decreased by circa 120m. Though the bars have different morphologies, they never grow oceanwards, due to the counteraction of the waves. Tide flows, on the contrary, are the main agents in the formation of the bars of the ebb tidal delta, on the boundary of the interaction of littoral drift and ebb flow.

The limit of action of littoral drift is situated at $d = H / 0.78$ (HARDISLY and LAVER, 1989), where d is depth (m) and H the wave mean height (m) when it brakes. Considering the wave mean breaker-height of 2.9m, during the period 2002-2003 (Instituto Hidrográfico data, 2003), the limit of action of littoral drift at the mouth would be at a depth of about 3.7m, estimated depth for the beginning of the ebb terminal lobe.

Presented hydrodynamic and sediment transport simulations results constitute a first attempt to understand the general behaviour of the bottom sediments in the Cávado River inlet under different river flows regimes and tidal conditions.

Waves, a key action in the sediment transport patterns, were not considered in the simulations. More detailed spatial information is needed in order to improve the simulations robustness. However, achieved results reasonably agree with observed data.

CONCLUSION

The morphological changes of the inlet cannot be considered in isolation. They are part of changes on the spit and on the coastal shore northwards.

From 1991 to 2003, the inlet maintained approximately the same configuration and aerial extent. It underwent small-scale changes associated with the formation and migration of swash bars and marginal channels. The ebb main channel has been located on the north side of the inlet, presenting a small migration to the SW when the flood tidal bar was located at the northern side. The spit platform has undergone some width, height and length changes. The breaching of the spit platform commonly occurs during storm conditions coincident with spring tides.

The present state of degradation of the breakwater on the northern side of the inlet, the reduced river flow and the absence of fluvial floods since 2001, would have contributed to an increase of the silting- up of the estuary.

The silting-up of the estuary decreases the channel depth. Consequently, the tidal prism and the capacity and competence of sedimentary transport by the currents have decreased. This generates a positive feedback that

progressively contributes to the infilling of the estuary. This progressive infilling and decrease of tidal prism reinforce the instability of the inlet, contributing to the collapse of estuarine ecosystems.

Presently, the Cávado inlet shows a continued infilling trend that increases with depth decrease. This fact is a risk for all type of boats, especially those of local fishermen.

Achieved results can be used as an important auxiliary source of information in order to select gauge stations for measurements of tidal water elevations, current velocity, and sediment concentrations. Once adequately calibrated, the developed models will constitute a powerful tool in assessing the bathymetric alterations under different hydrodynamic regimes, or to evaluate the efficiency of maritime works designed to protect Esposende and the sandy spit.

ACNOWLEDGEMENTS

We are grateful to APPLE and to Câmara Municipal de Esposende for their support to this study.
We would like to acknowledge Dr. Th. de Groot for his valuable contribution to the revision of this paper.

REFERENCES

ACKERS, P. and WHITE, W. R., 1973. Sediment Transport: New Approach and Analysis. *Journal of the Hydraulics Division*, American Society of Civil Engineers, No. HYll.

BENEVAVENTE J., GRACIA F. J. and LÓPEZ-AGUAYO F., 2000. Empirical model of morphodynamic beachface behaviour for low-energy mesotidal environments. *Marine Geology*, 167: 375-390.

BRUUN, P. and GERRITSEN, 1960. *Stability of coastal inlets*. North Holland Publ. Co., Amsterdam, 123 p.

BRUUN, P., GERRITSEN, F. and BHAKTA, N.P., 1974. Evaluation of overall entrance stability of tidal entrances. *Proc. 14th Conf. Coastal Engineering*, Copenaghen, 1566-1584.

CAMERON, W.M. and Pritchard, D.W. (1963). Estuaries. In: *The sea*. Vol. (II). M.N. Hill (ed) Interscience, New York. p306–324.

DAVIS, R.A. and HAYES, M. O., 1984. What is a wave dominated coast? *Marine Geology*, 60, 313-329.

DRUERY, B.M., DYSON, A.R. and GREENTREE, G.S. (1983). *Fundamentals of Tidal Propagation in Estuaries*. Proc. 6th Aust. Conf. Coastal and Ocean Engineering, 1983.

DYER, K.R.,1997. *Estuaries : a physical introduction*, Second Edition. J. Wiley and Sons Ltd., Chichester. 195pp.

FITZGERALD, D. M., 1984. Interactions between the ebb-tidal delta and landward shoreline: Price Inlet, South Carolina. *Journal of Sedimentary Petrology*, 4, 54,1303-1318.

GASSIAT, L., 1989. *Hydrodynamique et évolution sédimentaire d'un système lagune-fléche littorale (Bassin d Arcachon-Cap Ferret)*. Thèse de 3eme cycle, Université Bordeaux I, 228p.

GOODWIN, P., 1996. Predicting the stability of tidal inlet for wetland and estuary management. *Journal of Coastal Research*, S.I. 23, 83-102.

GORMAN L., MORANGO A., and LARSON R., 1998. Monitoring the coastal environment; Part IV: Mapping, shoreline changes, and bathymetric analysis. *Journal of Coastal Research*, 14(1), 61-92.

HARDISTY, J. and LAVER, A. J., 1989. Breaking waves on a macrotidal beach: a test of McGowan's criteria. *Journal of Coastal Research*, 5, 79-82.

HAYES, M. O., 1979. Barrier islands morphology as a function of tidal and waves regime. In: S. P. Leatherman (Ed.), *Barrier islands from the Gulf St Laurent to the Gulf of Mexico*, New York, Academic Press, 2,p. 1-28.

HENRIQUES, R., 2003. SEDMAC/SEDPC: programa informático de apoio à análise dimensional de populações detríticas. *Ciências da Terra,* Volume Especial, VI Congresso Nacional de Geologia, Faculdade e Tecnologia da Universidade Nova de Lisboa, p40.

JARRETT, J. T., 1976. Tidal prism-inlet area relationships. *GITI Rep. 3*, US Army CERC, Ft. Belvoir, Va., 32p.

KAMPHUIS, J. W., DAVIES, M. H., NAIRN, R. B. and SAYO, O. J., 1986. Calculation of litoral sand transport rate. *Coastal Engineering*, 10, 1-21.

KOMAR P. D. and GAUGHAN M. K., 1972. Airy wave theory and breaker height prediction. Proceedings of the 13th International Conference on Coastal Engineering ASCE, pp. 405-418.

MICHEL, D., 1993. *Dynamique sédimentaire en milieu littoral, évolution morphodynamique de la plage de la Salie*. Thèse d'État. Université de Bordeaux I, p. 24-25.

O'BRIEN, M. P., 1939. Tidal prism related to entrance areas. *Civil Engineering,* 1, 738-739.

PINHO, J. L. S., 2001. *Mathematical modelling application to hydrodynamics and water quality studies of coastal zones*. PhD Thesis. University of Minho, Braga, Portugal (in Portuguese)

PRITCHARD, D.W., 1955. Estuarine circulation patterns. *Proc. Am. Soc. Civ. Eng.*, **81**, No. 717.

JPL. A collection of global ocean tide models. Jet Propulsion Laboratory, Physical Oceanography Distributed Active Archive Center, Pasadena, CA; 1996. URL: http://podaac.jpl.nas.gov/

WES-HL, Users Guide To RMA2 Version 4.3, US Army Corps of Engineers - Waterways Experiment Station Hydraulics Laboratory, Vicksburg, USA (1996)

WES-HL, Users Guide To SED2D Version 4.5, US Army Corps of Engineers - Waterways Experiment Station Hydraulics Laboratory, Vicksburg, USA (2000)
--2002. Relatório de observações meteorológicas. Departamento de Pilotagem do Porto de Viana do Castelo.
--2003. Parâmetros da agitação marítima. Instituto Hidrográfico da Marinha, Lisboa.